

# Characteristics of UWB Propagation through Human Being behind a Wall

Kedar Nath Sahu, C. Dhanunjaya Naidu, and K. Jaya Sankar

**Abstract-**The detection and monitoring of cardiac activity using a radar has promising potential for through-the-wall detection applications. The objective of this paper is to calculate the UWB propagation losses that a radar signal suffers, when it is aimed at a human being behind the wall of a room. For this, an ultra-wideband (UWB) pulse propagation model is created to represent this real time scenario and simulated using CST Microwave Studio (MWS) to obtain the propagation parameters such as the reflection and transmission coefficients considering the incidence of an UWB signal in the frequency range 1-5 GHz. The outcome of this investigation may be useful in the design of a practical UWB radar meant for (i) measurement of heartbeat rate by a health doctor, (ii) non-invasive lie-detection and (iii) searching a person hidden in a room during criminal investigation. In addition, it is observed that, at specific frequencies, the variation of transmission coefficient has its relevance with the variation of heart size over a cardiac cycle.

**Index Terms-** Brick, Dielectric properties, Heartbeat rate, Reflection coefficient, Ultra-wideband propagation.

## I. INTRODUCTION

The detection and/or monitoring of heartbeat activity of human being using ultra-wideband radars are potentially used for applications which are based on the performance of human heartbeat. For measurement of heartbeat of a patient, the contact based methods require the physical contact with the human body and hence add to irritation due to discomfort during the measurement. Moreover, these methods also have the constraint that they depend on the accessibility of the affected part of the subject. So the need of detection and/or monitoring of cardiac performance using non-contact based methods like radars evolves as alternative means. In particular for lie detection applications the contact based methods suffer for being invasive. However, a non-contact based method like using a radar is non-invasive and suitable in case of inaccessible human subjects by placing the radar at a remote location, away from the subject under observation.

*Manuscript received Jan, 2018.*

**Kedar Nath Sahu**, Electronics and Communication Engineering, Stanley College of Engineering and Technology for Women, Hyderabad, India (e-mail: knsahu72@gmail.com).

**C. Dhanunjaya Naidu**, Electronics and Communication Engineering, VNR Vignana Jyothi Institute of Engineering and Technology, Hyderabad, India (e-mail: cdnaidu@yahoo.com).

**K. Jaya Sankar**, Electronics and Communication Engineering, Vasavi College of Engineering (Autonomous), Hyderabad, India (e-mail: kottareddyjs@gmail.com).

Another application of this radar based heartbeat detection could be useful for the search of a kidnapped person kept hidden in a room. Continuous-wave (CW) Doppler radars are used to measure the heartbeat rate from a distance. However, these measurements are limited due to their low penetrating ability through obstacles between the human body and the radar especially, for people hidden behind a wall. Ultra-wideband (UWB) radars and their models for heartbeat detection with direct exposure of UWB signal to the human being (i.e. without any obstacle between radar and the subject) have been described in [1-13]. In this work, using CST MWS, modeling and simulation were carried out for human body behind a brick wall.

In our earlier work [14], the model for human thorax (the part of the body between neck and waist) has been enhanced over the earlier models by including additional layers of air, skin in front of human being, and a layer of air at the back of a human being. In this work, an UWB propagation model of human being behind a brick wall is constructed and the propagation parameters such as impedance, reflection and transmission coefficients at various frequencies in the UWB range 1-5 GHz are estimated using CST Microwave Studio. The human body tissues and the brick wall material present between the human being and the radar have been modelled in order that the model reflects the actual structures of the materials and the electromagnetic processes involved in the propagation of the electromagnetic radiation through them. This model appears to be a real situation as shown in Figure 1. Further, the properties of various materials forming the layers vary with frequency and these variations have been taken into account while estimating the electromagnetic wave propagation behavior through these layers.

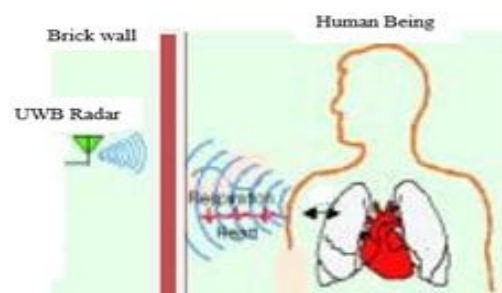


**Figure 1.** Human being behind a brick wall.

## II. THE METHODOLOGY

The procedural approach for this work involves the following steps.

- Study of the human thorax structure and the variation of heart size with time over one cardiac cycle.
- Study of the dielectric properties of dispersive materials.
- UWB pulse propagation model of human thorax behind a brick wall incorporating frequency dependent dielectric properties of the body tissues and wall materials.
- Use of CST Microwave Studio for calculation and analysis of the propagation performance parameters namely, system impedance, reflection and transmission coefficients.
- Study of the variation of transmission coefficient with time over one cardiac cycle.

## III. THE HUMAN THORAX STRUCTURE AND VARIATION OF HEART SIZE

When the thorax is illuminated by an RF signal emitted by a radar, the RF signal encounters various tissues partly or fully. This work uses a one-dimensional model of thorax considering some selected biological tissues such as skin, fat, muscle, cartilage, lungs and heart with reference to the human thorax slice [Figure 2] obtained from the Visible Human Project [15]. As seen from Figure 3, the upper part is the chest; the U-shaped left ventricle (LV) is found at the center left. The tissue layers seen from the chest to the heart are the skin and the fat (both yellowish), the muscle (red), the cartilage (reddish), the lung (red) and the heart wall (red). The pericardium is visible at the lung-heart boundary. The constitution of human heart and the cardiac cycle studied from the literature [16] is reported below.

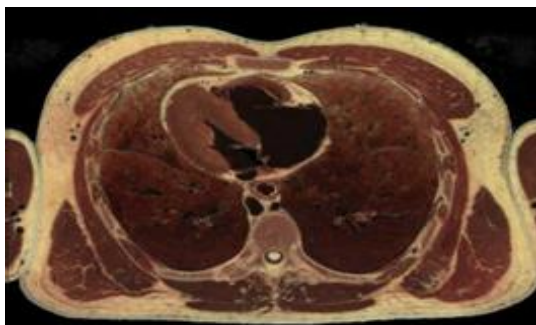


Figure 2. Human thorax slice of Visible Human Project.

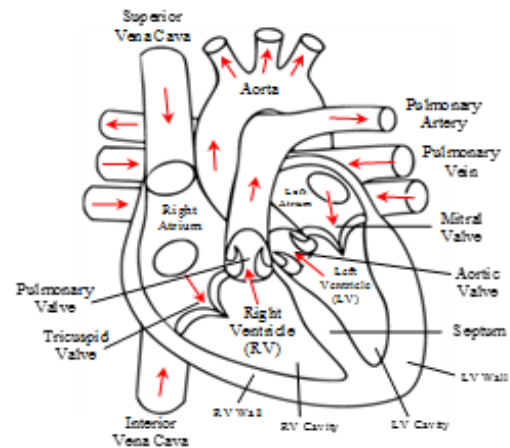


Figure 3. Transverse section of human heart.

The transverse cross-sectional view of the human heart structure is shown in Figure 3. Assuming the signal propagation from chest to back of the human body and with reference to Figure 3, the parts of the heart element encountering the path of propagation considered for the modelling are the LV wall, LV cavity, inter ventricular septum, RV cavity and RV wall. Both LV and RV are the longer cavities in the human heart. Moreover, the wall of LV is thicker than that of RV.

The function of human heart alternates between two phases: contraction (systole) and relaxation (diastole), in a concerted pattern known as a cardiac cycle. One cardiac cycle consists of one complete diastole followed by one complete systole. The duration of one complete systolic period is about 0.3 seconds and that of one complete diastolic period is 0.5 seconds. This contributes to one complete cardiac cycle of 0.8 seconds. On the basis of various investigations found in the literature, the human cardiac dimension and its variation with time in a cardiac cycle were studied and are reported below.

The left ventricle end diastole (LVED) is the length measured at the end of diastole (i.e. when the heart is completely dilated) and corresponds to the largest cardiac dimension. Similarly, the left ventricle end systole (LVES) is the length measured at the end of systole (i.e. when the heart is fully contracted) and is the smallest cardiac dimension. The ventricular free wall thickness, inter ventricular septum, the ventricular cavities (LV and RV), and their variations with time during a cardiac cycle have been measured by using several methods such as echocardiography, angiography, cine MRI etc. as reported in [17-22].

Based on the changes of cavity dimension, wall thickness with time as well as their peak rates of change as reported in [23], the instantaneous values of the total transverse dimension of heart (in millimeter) during the systole and diastole are determined for one complete cardiac cycle of 0.8 seconds as shown in Figure 4. These instantaneous dimensions of heart are used for the analysis of the model.

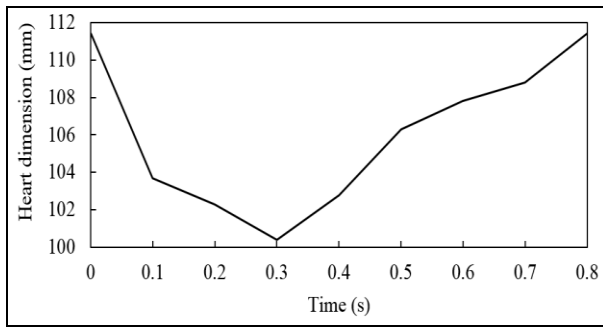


**Figure 4.** Variation of human heart thickness with time over a cardiac cycle.

When an RF signal is exposed to a human being behind a wall, the EM wave propagation behaviour is greatly modified when it passes through the human body tissues and building wall material. This is because, the composite system of the brick wall and human body consists of irregular, inhomogeneous, lossy and frequency dependent dielectric materials. Keeping this in view, literature survey was made on the dielectric properties of dispersive materials as presented in Section IV.

#### IV. DIELECTRIC PROPERTIES OF DISPERSIVE MATERIAL MEDIA

A medium in which the parameters such as permittivity, conductivity etc. that affect the propagation of an EM wave vary with frequency is called a dispersive medium [24]. In most of the materials, the magnetic response is usually weaker than the dielectric response [25] and therefore, for loss calculation in a dispersive dielectric medium, only wave modifications due to the dielectric constant  $\epsilon_r$  becomes significant. As the human body tissues as well as the building materials are the components of the EM propagation model used in this work, the frequency dependence of their dielectric properties found in the literature is reported below.

##### 4.1. Frequency Dependent Dielectric Properties of Human Body Tissues

The dielectric properties of human body tissues at radio frequencies have been studied by several investigators. In the case of biological tissues, the permittivity depends on the type of tissues. Tissues having more water content, for example, heart, muscle, kidney, brain, liver, pancreas etc. have larger dielectric constant and effective conductivity than the tissues of low water content such as fat, bone and lung [26]. In general, the dielectric constant of tissues decreases with increase in frequency over a wide range of frequencies. On the other hand, the effective conductivity increases with frequency more rapidly beyond 1 GHz. The mathematical expression (1) known as the Cole and Cole equation [27] describes the dispersive behavior of human body tissues.

$$\epsilon_c(\omega) = \epsilon'(\omega) - j\epsilon''(\omega) = \epsilon_\infty + \sum_{n=1}^4 \frac{\Delta\epsilon_n}{1 + (j\omega\tau_n)^{1-\alpha_n}} + \frac{\sigma_s}{j\omega\epsilon_0}, \quad (1)$$

where  $\epsilon_\infty$  is the optical dielectric constant;  $\epsilon_0$  refers to the

dielectric constant of vacuum;  $\tau_n$  represents the relaxation time constant of the tissue;  $\alpha_n$  denotes a distribution parameter;  $\sigma_s$  is the static conductivity and  $\Delta\epsilon_n = \epsilon_s - \epsilon_\infty$ , the deviation between the static dielectric constant  $\epsilon_s$  and the optical dielectric constant  $\epsilon_\infty$ .

The frequency dependent dielectric properties according to the four term Cole-Cole model described in (1) for various human tissues based on the data compiled by Gabriel have been computed from 10 Hz to 100 GHz [28].

##### 4.2. Frequency Dependence of the Dielectric Properties of Building Wall Materials

The materials with which the wall is made up of, are lossy at high frequencies. This is not only because they exhibit a finite conductivity  $\sigma$  but also due to their complex permittivity  $\epsilon_c = \epsilon' - j\epsilon''$ . Often, for a lossy dielectric material, the electrical properties are represented by real permittivity  $\epsilon'$  and the loss tangent  $\tan\delta$  such that,  $\tan\delta = \sigma_{eff}/\omega\epsilon' = \epsilon''/\epsilon_r'$  where  $\sigma_{eff}$  is the effective conductivity and is equal to  $\omega\epsilon''$ .

In general, moisture content, density, homogeneity and porosity are the important factors to determine their dielectric properties. The EM parameters commonly used to represent the propagation characteristics through materials are the dielectric constant, loss tangent, conductivity, insertion loss, return loss, path loss or propagation loss, reflection coefficient and transmission coefficient and are obtained from various theoretical and experimental techniques as reported in [29-35]. Recent studies have been conducted on the characterization of wall materials [36-38] over the UWB range 3.1 to 10.6 GHz. The wall thickness is the critical parameter in the event of characterization of wall materials which are exposed to the RF signal.

Concrete and brick are the most popular building construction materials. For the assessment of signal dispersion and attenuation through a wall material, accurate data of complex dielectric constant of the material is a must. According to [39], it may not be possible to obtain a specific trend in the variation of the dielectric properties. So, often, the wall-made material is characterized as a dielectric material of effective permittivity  $\epsilon'$  and conductivity  $\sigma = \omega\epsilon''$  constant over a range of frequencies so that the choice of having  $\epsilon''$  inversely proportional to any frequency in the range can be achieved, according to [40]. The thickness and dielectric constant of typical wall materials commonly used in building environments: dry wall, wooden door, brick and concrete block at 5 GHz found in [41] are listed in Table 1.

**Table 1.** Thickness and dielectric constant of dry wall, wooden door, brick and concrete block.

Material	Thickness (cm)	$\epsilon_r'$	Frequency range (GHz)
Dry wall	1.16992	2.44	0.6 - 13.9
Wooden door	4.44754	2.08	1.0 - 14.3
Brick	8.71474	4.22	1.0 - 7.0
Concrete block	19.45	2.22	2.0 - 6.8


A comparison of these results indicates that they are sufficiently accurate. It is also reported in [41] that, for most of the materials, the measurement of the loss tangent is a more difficult task than the measurement of the real part of complex relative permittivity  $\epsilon_r'$ . However, as the insertion loss of a wall is mainly due to the reflection and is negligibly less due to the absorption of the RF signal energy, the inaccuracies in the values of loss tangents hardly impacts the evaluation of the path loss.

The experimental data obtained by the Office National d'Etudes et de Recherches Aérospatiales (ONERA), a French aerospace research agency for the complex relative permittivity of brick (20 cm thick) over the ultra-wideband

frequency range 1 - 5 GHz is  $\epsilon_r = 5.0-j0.45$  [42] and has been used for modelling purpose in this work.

## V. MODELLING AND SIMULATION OF HUMAN BEING BEHIND A BRICK WALL

The composite system of a human being behind a wall made up of brick material is modelled as a planar multilayered structure of the entire media through which the UWB pulse propagation takes place. The dimensional thicknesses and the dielectric properties of various human body tissues and brick wall are mentioned in Section 4.1.

AIR	SKIN	FAT	MUSCLE	CARTILAGE	LUNG	HEART	CARTILAGE	MUSCLE	FAT	SKIN	AIR
1000	1.5	9.6	13.5	11.6	5.78		11.6	13.5	9.6	1.5	

**Figure 5.** Planar layered model of human being behind a brick wall – forward and backward propagations. The numbers in the diagram indicate the thickness of the tissue layers in millimeters.

### 5.1. Modelling

The planar layered structure of the model is shown in Figure 5. The values of relative permittivity (*Epsilon*)  $\epsilon_r$  and electrical conductivity (*El. conductivity*)  $\sigma$  for brick required to be inputted for simulation using CST MWS have been obtained (corresponding to the center frequency 3 GHz) from its complex permittivity,  $\epsilon_r = 5-j0.45$ . The dielectric properties for various materials used in this model are shown in Table 2.

**Table 2.** Epsilon and El. conductivity for human body tissues and brick material used in the model at 3 GHz.

Tissues	Epsilon	El. conductivity
skin	38.8	1.74
fat	10.85	0.34
muscle	53.6	2.14
cart	39.85	2.2
lung	49.2	2.1
heart	56.2	2.73
brick	5.02	0.075

The planar multilayered model shown in Figure 5 is simulated in the UWB frequency range 1 to 5 GHz. The results of propagation losses are presented and discussed in Section 5.2.

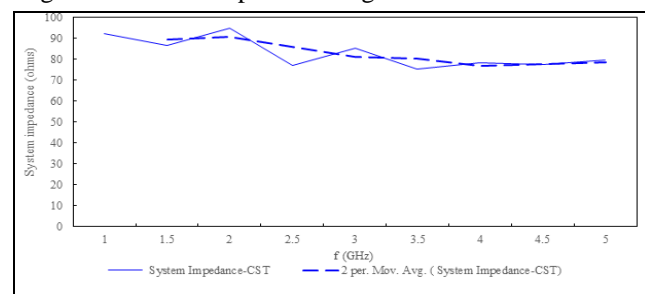
### 5.2. Simulation Results and Discussion

The simulation is carried out for the model considering the deflated state of the human heart. The results of simulations using CST MWS for the parameters such as impedance, reflection and transmission coefficients are presented below.

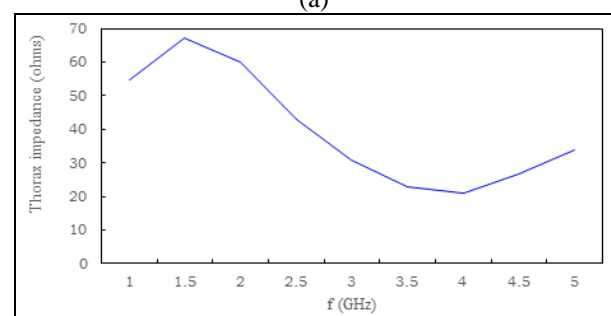
#### 5.2.1. Impedance:

The impedance offered by the entire composite structure of the brick wall - air - human body - air is defined as the system

impedance (ohms). The system impedance as well as the thorax impedance (impedance offered by the human thorax alone) obtained for the dilated heart at specific frequencies are obtained and their variations with frequency in the UWB range 1-5 GHz are depicted in Figure 6.



(a)



(b)

**Figure 6.** Variation of (a) system impedance (ohms) and (b) thorax impedance (ohms) with frequency considering dilated heart.

It is observed that both system impedance as well as thorax impedance are less than the impedance of free space at any specific frequency in the band 1 to 5 GHz.

#### 5.2.2. Reflection Coefficient:

The reflection coefficients (dB) are obtained for the dilated heart at specific frequencies in the range 1-5 GHz. The

variation of reflection coefficients (dB) with frequency is plotted in Figure 7.

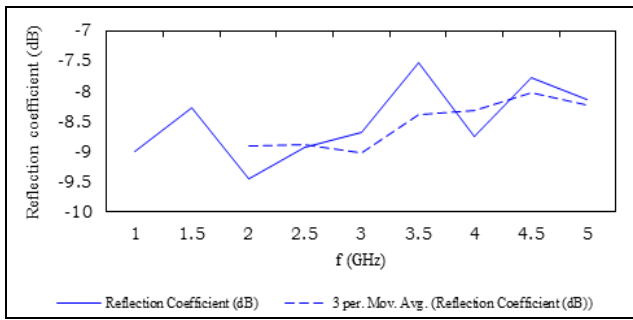


**Figure 7.** Variation of reflection coefficient (dB) with frequency for the dilated heart. The moving average values are also plotted.

5.2.3. *Transmission Coefficient:*

The transmission coefficients (dB) are obtained for the model of human being behind a brick wall at selected discrete frequencies in the UWB range 1-5 GHz for the varying dimensions of the heart corresponding to the systole and diastole periods of one cardiac cycle. However, the variation of transmission coefficient at frequencies 1.5, 2, 2.5 and 3 GHz are shown [Figure 8] since the transmission coefficient variation follows the variation of heart dimension during the cardiac cycle, only at these specific discrete frequencies.

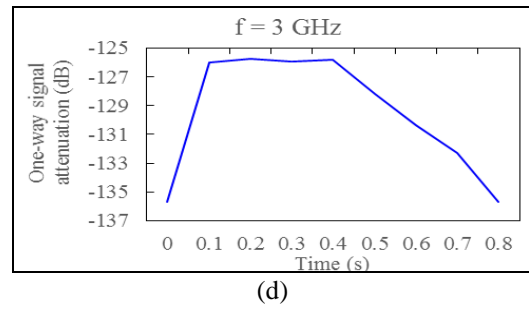
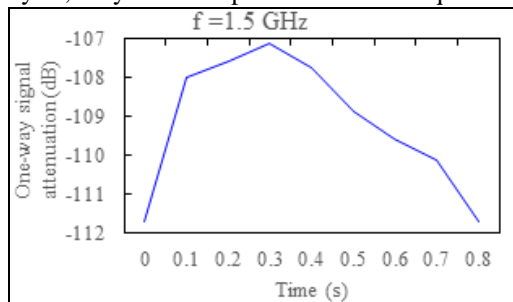


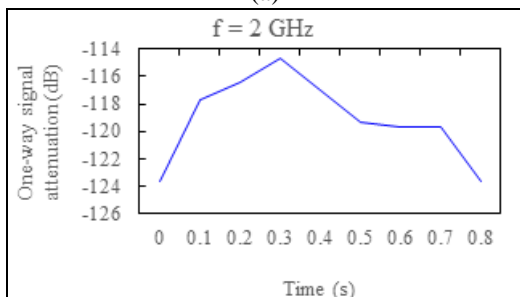
**Figure 8.** Variation of transmission coefficient with time at specific frequencies (a) 1.5 GHz (b) 2 GHz (c) 2.5 GHz and (d) 3 GHz.

Thus it is observed that the variation of transmission coefficient in a cardiac cycle is in tune with the variation of the cardiac dimension both in systole (up to 0.3 seconds) and diastole (0.3 to 0.8 seconds) periods of the cardiac cycle at 1.5, 2, 2.5 and 3 GHz [Figure 8]. During the cardiac systole, the transmission coefficient decreases as the heart dimension decreases and the same increases with the heart dimension during the cardiac diastole. The variation of transmission coefficient repeats itself for every subsequent beating of heart and this is in tune with the heartbeat rate of a human being present behind a wall. This indicates that there is a periodic variation in the transmission coefficient of an active heart at these specific frequencies. The periodicity between the adjacent maxima or minima of the transmission coefficient characteristics is a sign of the heartbeat period.

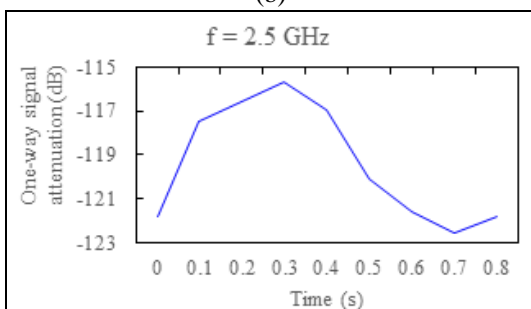
The variations of maximum and minimum transmission coefficients (dB) with frequency are shown in Figure 9. It is observed that the periods of maximum and minimum attenuation vary with frequency.



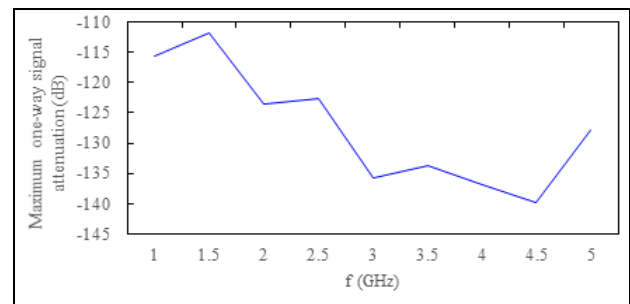
(a)



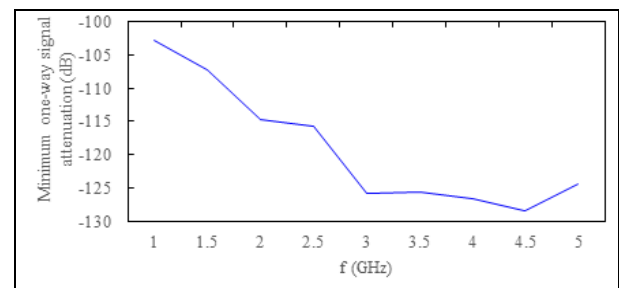
(b)



(c)



(a)



(b)

**Figure 9.** Variation of (a) maximum and (b) minimum transmission coefficient (dB) with frequency.

## I. CONCLUSIONS

In this work, the impedance, reflection and transmission coefficient are estimated from the simulation of propagation characteristics of EM waves through the multilayered structure of a human being behind a brick wall using CST MWS. The frequency dependent properties of various layers are taken into account for all calculations.

It has been observed that at any frequency in the band 1 to 5 GHz, the system impedance is less than the impedance of free space. This is in consistent with the principle of electromagnetics in order to get possible reflection of the signal transmitted. Additionally, at specific frequencies of 1.5, 2, 2.5 and 3 GHz, the transmission coefficients (dB) for the varying heart dimensions closely follow the variation of heart during the cardiac cycle. This pattern of variation of transmission coefficient (dB) repeats itself for every subsequent beating of heart and is in tune with the heartbeat of a human being. This aspect reflects some possible sign *that can be used as the indicator of the state of the heart of a human being*. The outcome of this work may be useful for the design of a practical radar that can be mounted outside the wall of a room, possibly for three important areas of applications like (i) study of health of a human patient, (ii) criminal investigation (or lie detection), and (iii) search and rescue of person hidden in a room. However, the relation between the variation of transmission coefficient and that of heart size in view of any possible heartbeat detection need to be ascertained by further intensified research.

## REFERENCES

- [1] L. Anitori, A. de Jong and F. Nennie, *FMCW radar for life-sign detection*, 2009 IEEE Radar Conf., Pasadena, CA, (2009), 1- 6.
- [2] T. Berger, S. E. Hamran, L. Hanssen and M. J. Øyan, "Ultra-Wideband Radar Design for Detection of Vital Signs," NATO RTO/SET-125 Symp. Defence Against Terrorism, April 2008.
- [3] C. G. Bilich, Bio-medical sensing using ultra-wideband communications and radar technology: A feasibility study, Pervasive Health Conf. and Workshops 2006, **29** (2006), 1–9.
- [4] C. G. Bilich, *Feasibility of dual UWB heart rate sensing and communications under FCC power restrictions*, 3rd Int. Conf. Wireless and Mobile Commun. 2007 (ICWMC 2007), Guadaloupe, French Caribbean, (2007).
- [5] I. Y. Immoreev, S. Samkov and T. H. Tao, *Short-distance UWB radars*, IEEE Aerosp. Electron. Syst. Mag., **20** (6) (2005), 9–14.
- [6] I. Immoreev, and T. H. Tao, *UWB radar for patient monitoring*, IEEE Aerosp. Electron. Syst. Mag. **20** (2008), 11-18.
- [7] S. N. Pavlov and S. V. Samkov, *Algorithm of signal processing in ultra-wideband radar designed for remote measuring parameters of patient's cardiac activity*, 2004 2nd Int. Workshop Ultra-wideband and Ultra-short Impulse Signals 2004, Sevastopol, (2004), 205–207.
- [8] S. Pisa, P. Bernardi, M. Cavagnaro, E. Pittella and E. PiuZZi, *Monitoring of cardio-pulmonary activity with UWB radar : a circuital model*, Proc. 2008 Asia-Pacific Symp. Electromagn. Compatibility and 19th Int. Zurich Symp. Electromagn. Compatibility, Singapore, (2008), 224-227.
- [9] N. V. Rivera, S. Venkatesh, C. Anderson and R. M. Buehrer, *Multi-target estimation of heart and respiration rates using ultra-wideband sensors*, 14th European Signal Process. Conf., Florence, Italy, (2006), 1-6.
- [10] E. M. Staderini, UWB radars in medicine, IEEE Aerosp. Electron. Syst. Mag. **17** (1) (2002), 13–18.
- [11] E. M. Staderini and G. Varotto, *Optimization criteria in the design of medical UWB radars in compliance with the regulatory masks*. IEEE Biomed. Circuits Syst. Conf. (BIOCAS 2007), Montreal, Que, (2007), 53–58.
- [12] G. Varotto and E. M. Staderini, *On the UWB medical radars working principles*, Int. J. Ultra-Wideband Commun. Syst. **2** (2011), 83-93.
- [13] A. G. Yarovoy, L. P. Lighthart, J. Matuzas and B. Levitas, *UWB radar for human being detection*, IEEE Aerosp. Electron. Syst. Mag. **23** (5) (2008), 36–40.
- [14] K. N. Sahu, C. D. Naidu, M. Satyam and K. Jaya Sankar, *Study of RF signal attenuation of human heart*, J. Eng., Hindawi Publishing Corporation, **2015** (2015), 1-8. (ISSN: 2314-4904) doi: 10.1155/2015/484686.
- [15] Y. J. Chang, "The NPAC visible human viewer," Syracuse University, New York, 1997.
- [16] S. Standring, "Gray's Anatomy: The Anatomical Basis of Clinical Practice, Expert Consult," 40th ed., Elsevier, 2009.
- [17] D. G. Gibson, T. A. Trail and D. J. Brown, Changes in left ventricular free wall thickness in patients with ischaemic heart disease, British Heart J. **39** (1977), 1312-1318.
- [18] K. Hergan, A. Schuster, M. Mair, R. Burger and M. Topker, Normal cardiac diameters in cine-MRI of the heart, R'oFo:Fortschritte auf dem Gebiete der R'ontgenstrahlen undder Nuklearmedizin, **176** (11) (2004), 1599 –1606.
- [19] L. E. Hudsmith, S. E. Peterson, J. M. Francis, M. D. Robson and S. Neubaner, *Normal human left and right ventricular and left atrial dimension using steady state free precession magnetic resonance imaging*, J. Cardiovascular Magn. Resonance, **7** (2005), 775-782.
- [20] S. Kaul, G. L. Wismer, T. J. Brady, D. L. Johnston, A. E. Weyman, R. D. Okada and E. Dinsmore, *Measurement of normal left heart dimensions using optimally oriented MR images*, American Roentgen Ray Society, **146** (1986), 75-79.
- [21] R. F. Rushmer and N. Thal, *The mechanics of ventricular contraction: A cinefluorographic study*, J. American Heart Assoc. **4** (1951), 219-228.
- [22] T. A. Traill, D. G. Gibson and D. J. Brown, Study of left ventricular wall thickness and dimension changes using echocardiography, British Heart J. **40** (1978), 162-169.
- [23] D. G. Gibson, T. A. Trail and D. J. Brown, Changes in left ventricular free wall thickness in patients with ischaemic heart disease, British Heart J. **39** (1977), 1312-1318.
- [24] W. H. Hayat and J. A. Buck, "Engineering Electromagnetics," 7th ed., India: Tata McGraw-Hill, 2006.
- [25] M. N. Afsar, J. R. Birch and R. N. Clarke, *The measurement of the properties of materials*, Proc. IEEE. **74** (1) (1986), 183-199.
- [26] U. S. Inan and A. S. Inan, "Engineering Electromagnetics," 1st ed. India: Pearson Education Inc. 2010.
- [27] S. Cole and R. H. Cole, Dispersion and absorption in dielectrics: I. Alternating current characteristics, J. Chem. Phys. **9** (1941), 341–351.
- [28] C. Gabriel, "Compilation of the dielectric properties of body tissues at RF and microwave frequencies," Occupational and environmental health directorate, radio freq. radiation division, Brooks Air Force Base, Texas, USA. Rep. N.AL/OE-TR-1996-0037, 1996.
- [29] J. Baker-Jarvis, E. J. Vanzura and W. A. Kissick, *Improved technique for determining complex permittivity with the transmission/reflection method*, IEEE Trans. Microw. Theory Techn. **38** (8), (1990), 1096-1103.
- [30] T. Gibson and D. Jenn, *Prediction and measurements of wall insertion loss*, IEEE Trans. Antennas Propag. **47** (1) (1999), 55-57.
- [31] A. Gulck, T. Lehmann and R. Knochel, *Characterization of dielectric obstacles using ultra-wideband techniques*, 35th European Microw. Conf., **3** (2005).
- [32] U. C. Hasar and O. Simsek, *An accurate complex permittivity method for thin dielectric materials*, Progress Electromagn. Res. **91** (2009), 123-138.
- [33] U. C. Hasar and C. R. Westgate, A broadband and stable method for unique complex permittivity determination of low-loss materials, IEEE Trans. Microw. Theory Techn. **57** (2009), 471-477.
- [34] H. Hashemi, *The indoor propagation channel*, Proc. IEEE, **81** (7) (1993), 943-968.
- [35] N. Jebbor, S. Bri, A. Nakheli, L. Bejjit, M. Haddad, and A. Mamouni, *Complex permittivity determination with the transmission/reflection method*, Int. J. Emerg. Sci. **1** (4) (2011), 682-695.
- [36] J. Y. Lee and S. Choi, *Through – material propagation characteristics and time resolution of UWB signal*, Int. Workshop on Ultra-Wideband Systems, 2004 Joint with Conf. Ultra-Wideband Syst. and Technol. 2004 (IWUWBS 2004 and UWBST 2004), (2004), Kyoto, Japan, 71-75.
- [37] C. Liu, C. Huang and C. Chiu, Channel capacity for various materials of partitions in indoor ultra-wideband communication system with multiple input multiple output, 3rd IEEE / FIP Int. Conf. Central Asia on Internet 2007 (ICI 2007), Tashkent, (2007), 1-5.
- [38] A. H. Muqaibel, A. Safaai-Jazi, A. Bayram, A. M. Attiya and S. M. Riad, *ultra-wideband through-the-wall propagation*, Proc. IEE Microw. Antennas Propag. **152** (6) (2005), 581-588.

- [39] I. Cuinas and M. G. Sanchez, *Measuring, modeling, and characterizing of indoor radio channel at 5.8 GHz*, IEEE Trans. Veh. Technol. **50** (2) (2001), 526-535.
- [40] A. Ogunsla, U. Reggiani and L. Sandrolini, *Shielding effectiveness of concrete buildings*, IEEE 6th Int. Symp. Electromagn. Compatibility Electromagn. Ecol. 2005, Saint Petersburg, Russia, (2005), 65-68.
- [41] M. G. Amin, "Through-The-Wall Radar Imaging," Taylor and Francis Group, FL: CRC Press, 2011.
- [42] N. Maaref, P. Millot, C. Pichot and O. Picon, *A study of UWB FMCW radar for the detection of human beings in motion inside a building*, IEEE Trans. Geosci. Remote Sens. **47** (5) (2009), 1297-1300.

national, international journals and conferences. He is a Senior Member IEEE and a Fellow of IETE and IE (India), Life member of SEMCE (India) and ISTE.



**Kedar Nath Sahu**, Professor, Department of Electronics and Communication Engineering, Stanley College of Engineering and Technology for Women, Hyderabad, India, received the professional engineering degrees in Electrical Engineering (1996) and Electronics and Communication Engineering (2001) from The Institution of Engineers (India) and M.Tech. (2002) from Visvesvaraiyah Technological University, Karnataka, India. He received Ph.D. Degree in Electronics and Communication Engineering from Jawaharlar Nehru Technological University Hyderabad (JNTUH), Hyderabad in 2017. He has over 16 years of experience in teaching in the faculty of Electronics and Communication Engineering at various engineering colleges. His research interests include Applied Electromagnetics, Biomedical Engineering, Microwave and Radar Engineering. He is Fellow IETE, IE (India) and Life Member of ISTE.



**C. Dhanunjaya Naidu**, Professor, Department of Electronics and Communication Engineering, VNR Vignana Jyothi Institute of Engineering and Technology, Hyderabad, India received B.Tech. in Electronics and Communication Engineering (1982) and M.Tech. degree in 1985 from the College of Engineering, S. V. University, Tirupati, Andhra Pradesh, India. He earned his Ph.D. Degree in Electronics and Communication Engineering from JNTUH, Hyderabad. He has published several research papers in various national, international journals and conferences. His research interests include Signal Processing, Image Processing, and Neural Networks. He is a Fellow of IE (India), IETE and Life Member of ISTE.



**K. Jaya Sankar**, Professor and Head, Department of Electronics and Communication Engineering, Vasavi College of Engineering, Hyderabad, India, received B.Tech degree in Electronics and Communication Engineering from S. V. University, Tirupati, India and M.E. and Ph.D. degrees from the Department of Electronics and Communication Engineering, Osmania University, Hyderabad, India in 1988, 1994, and 2004 respectively. After a brief stint in a few industries, he joined Vasavi College of Engineering, Hyderabad in the year 1992.

He has 24 years of experience in teaching Electromagnetics, Antennas and Wave Propagation, Digital Communication and Microwave and Radar Engineering. His research areas of interest are in Coding Theory, RF and Wireless Communications and Genetic Algorithm based antenna design. He has published more than 50 research papers in